Nanoscale Advances

ROYAL SOCIETY OF CHEMISTRY

COMMUNICATION

View Article Online
View Journal | View Issue

Cite this: *Nanoscale Adv.*, 2025, **7**, 4293

Received 11th March 2025
Accepted 27th May 2025

DOI: 10.1039/d5na00234f

rsc.li/nanoscale-advances

Antibacterial gold nanoclusters combined with meropenem for the treatment of sepsis by alleviating the cytokine storm†

Chengli Wen, ‡[ab] Youkun Zheng, ‡[c] Yong Li,[de] Liping Yuan,[fg] Sicheng Liang,[bf] Xianying Lei,[a] Tao Xu,[a] Qinxue Hu,[a] Yuan Li,[a] Muhan Lü,*[bf] Wanmeng Xiao*[bfh] and Zehui Yu*[bi]

Sepsis is a life-threatening condition characterized by systemic organ dysfunction caused by a cytokine storm mediated by inflammatory mediators. Antibacterial gold nanoclusters (AuDAMP) were synthesized *via* a one-pot method. The therapeutic efficacy of AuDAMP was systematically evaluated in two sepsis mouse models: the cecum ligation and puncture (CLP) model and the lipopolysaccharide (LPS)-induced sepsis-associated acute lung injury model. Remarkably, AuDAMP demonstrated potent anti-septic effects through antimicrobial activity and attenuation of the cytokine storm. Furthermore, AuDAMP exhibited synergistic therapeutic effects when combined with meropenem, suggesting great potential as a novel therapeutic strategy for sepsis management.

Sepsis is a life-threatening condition resulting from organ dysfunction caused by a dysregulated host response to infection.[1] It is a significant global healthcare challenge, affecting millions of people annually and resulting in mortality rates ranging from one-sixth to one-third of those afflicted.[2] Despite advancements in medical technology, the success rate of sepsis management has improved, yet many patients still succumb to this condition. The major contributor to sepsis-related mortality is a severe cytokine storm, which leads to immune dysfunction and multiorgan failure.[3] Severe cytokine storm results from dysregulated inflammatory responses, posing a significant challenge for clinicians. This inflammatory dysregulation is typically initiated and driven by the overactivation of toll-like receptors (TLRs), which recognize and bind to pathogen-associated molecular patterns (PAMPs) or damage-associated molecular patterns (DAMPs).[4] TLRs recognize various inflammatory mediators, such as bacterial lipoproteins, lipopolysaccharides (LPSs), and double-stranded RNA (dsRNA). These interactions activate the intracellular transcription factor nuclear factor-kappa-B (NF-κB), leading to the induction of proinflammatory cytokines such as interleukin-1β (IL-1β), interleukin-6 (IL-6), and tumor necrosis factor-α (TNF-α), as well as procoagulants and adhesion molecules. The aberrant production of these substances triggers a cytokine storm.[5–8] Reducing the cytokine storm and controlling the underlying causes of inflammatory dysregulation are crucial for effectively managing and treating sepsis.

Traditional antimicrobial resistance is often linked to treatment failure and the recurrence of infections.[9] Rapid advances in nanomedicine are promising for the treatment of sepsis and drug-resistant bacteria. Nanomaterials serve not only as carriers for drug delivery but also as nanoantibiotics, offering innovative approaches to combat these challenging conditions.[10–12] Instead of seeking new traditional antibiotics, many researchers are concentrating on developing emerging nanoantimicrobials or utilizing nanotechnology to enhance the bactericidal effects of existing antibiotics.[13–15]

Gold is highly inert and stable, and gold-based nanoclusters (Au NCs) have demonstrated biocompatibility in animal models.[16–18] Recent studies have shown that ultrasmall Au NCs constitute a class of innovative nanoantibiotics that show great

[a]*Department of Critical Care Medicine, The Affiliated Hospital, Southwest Medical University, Luzhou 646000, China. E-mail: lvmuhan@swmu.edu.cn; Tel: +86-0830-3162122*

[b]*Human Microecology and Precision Diagnosis and Treatment of Luzhou Key Laboratory, Luzhou 646000, China. E-mail: hello_xwm@hotmail.com; yuzehui_swmu@outlook.com; Tel: +86-18227589096; +86-18111520223*

[c]*Basic Medicine Research Innovation Center for Cardiometabolic Diseases, Ministry of Education, Southwest Medical University, Luzhou 646000, China*

[d]*Department of Anesthesiology, People's Hospital of Naxi District, Luzhou 646000, China*

[e]*Department of Anesthesiology, Luzhou People's Hospital, Luzhou 646000, China*

[f]*Department of Gastroenterology, The Affiliated Hospital, Southwest Medical University, Luzhou 646000, China*

[g]*Department of Gastroenterology, The First People's Hospital of Liangshan Yi Autonomous Prefecture, Xichang 615000, China*

[h]*The Clinical Medicine Research Center, The Affiliated Hospital, Southwest Medical University, Luzhou 646000, China*

[i]*Laboratory Animal Center, Southwest Medical University, Luzhou 646000, China*

† Electronic supplementary information (ESI) available: Supplementary files including Fig. S1. characteristics of AuDAMP and Fig. S2. effects of AuDAMP on liver and kidney function in normal mice. See DOI: https://doi.org/10.1039/d5na00234f

‡ Chengli Wen and Youkun Zheng contributed equally to the study.

potential for application in combating multidrug-resistant bacterial infections.[19,20] The primary antimicrobial mechanism of ultrasmall Au NCs involves the disruption of cell membranes and the induction of cellular damage. Studies indicate that Au NCs smaller than 2 nm can easily penetrate cells, aiding in the eradication of intracellular bacteria.[20,21] Therefore, ultrasmall Au NCs exhibit antimicrobial activity against both intracellular and extracellular bacteria. Research by Fang-Hsuean Liao *et al.* revealed that subnanometer gold clusters can adhere to Lipid A, offering protection against LPS-induced sepsis.[22] Ultrasmall Au NCs have the potential to bind LPS, thereby reducing plasma LPS levels and mitigating LPS-induced sepsis while maintaining antimicrobial activity. This dual function makes them promising tools in the fight against sepsis.[22] In our previous work, broad-spectrum antibacterial ultrasmall Au NCs were synthesized *via* a one-pot method, with 4,6-diamino-2-mercaptopyrimidine (DAMP) serving as both surface ligands and reducing agents.[21] It remains unclear whether AuDAMP attenuates the inflammatory response and reduces mortality in sepsis or if it enhances antiseptic effects when used in combination with antibiotics. We hypothesize that AuDAMP may mitigate the cytokine storm and organ damage through its antimicrobial and LPS-scavenging properties in sepsis. Additionally, it could be used in combination with antibiotics to enhance antiseptic activity.

In this study, DAMP is a derivative of 2-mercaptopyrimidine with no direct pharmacological effect and can be used as a predrug for the preparation of nanoantibiotics.[23] AuDAMP was synthesized according to our previously reported approach called one-pot method.[24] The prepared AuDAMP appeared mustard-like (inset 1) and exhibited red photoluminescence (inset 2) under visible and UV light (Fig. S1A†), respectively. Fig. S1A† shows that the emission and photoluminescence excitation are centered at 770 nm and 450 nm, respectively, and the Stokes shift is as high as 200 nm. Fig. S1B† shows the UV-vis absorption spectrum of the prepared AuDAMP, which shows no characteristic plasmon resonance peaks in the UV region, which is consistent with the successful formation of Au NCs rather than large-sized nanoparticles. Fourier transform infrared spectroscopy results confirm DAMP anchoring to the AuDAMP surface (Fig. S1C†). We analysed the structural characteristics of AuDAMP by mass spectrometry. Mass spectroscopy was performed on a matrix-assisted laser desorption/ionization time-of-flight mass spectroscopy (MALDI-TOF MS) 4800 plus mass spectrometer (Applied Biosystems). The molecular formula of the as-prepared AuDAMP was also further clarified using MALDI-TOF mass spectrometry analysis. The data show that Au_{13} clusters are the major species in AuDAMP solutions, including the highly abundant formulas $[Au_{13}(DAMP)_5]^{4-}$ and $[Au_{13}(DAMP)_6]^{4-}$, and other formulas such as $[Au_9(DAMP)_9]^{3-}$, $[Au_{12}(DAMP)_9]^{3-}$, and $[Au_{17}(DAMP)_6]^{4-}$ are also present (Fig. S1D†). Particle size of AuDAMP was calculated based on the TEM images. This method is widely used.[19,20,25,26] As shown in Fig. S1E,† the TEM image revealed that AuDAMP was dispersed in ultrasmall clusters with a statistically significant average size of 1.8 ± 0.3 nm (inset) (100 particle sizes were measured with ImageJ, and their means and standard deviations were calculated). The ζ-potential of AuDAMP reached +38.4 mV, which indicates that it has good colloidal stability in aqueous solution. Therefore, the positive charge of AuDAMP suggests that it may interact with negatively charged bacteria as well as negatively charged free LPS in aqueous solution, thus binding bacteria and LPS, killing bacteria and decreasing free LPS.[13,21,27] Fig. S1F† shows the binding energies of Au $4f_{7/2}$ and Au $4f_{5/2}$ at 83.8 eV and 87.6 eV, respectively, indicating the coexistence of Au(I) and Au(0) in AuDAMP.

Moreover, animal experiments were conducted. All experiments were conducted in accordance with the guidelines for animal experimentation and were approved by the Animal Ethics Committee of Southwest Medical University (approval number: swum.20240040). The animals were fed in a specific pathogen-free (SPF) environment at Southwest Medical University, with the temperature maintained between 21 °C and 25 °C, a 12-hour light/dark cycle, and unrestricted access to food and clean water. The mice did not exhibit any unexpected deaths during the study. Study 1: establishing and grouping the cecum ligation and puncture (CLP)-induced sepsis model. The mice were randomly divided into seven groups: Sham, CLP, CLP_AuDAMP1, CLP_AuDAMP2, CLP_AuDAMP3, CLP_mlpn (mlpn stands for meropenem), and CLP_AuDAMP3_mlpn. The mice were anesthetized with tribromoethanol, and their abdomens were shaved and sterilized with 75% alcohol. After the limbs of the mice were secured with tape, half of the cecum was ligated, and the distal cecum was punctured with a 22-gauge needle. An equal amount of faeces was extruded to establish a polymicrobial infection sepsis model. After the sepsis model was established, each mouse received an intraperitoneal injection of 1 ml of saline and was resuscitated on a rewarming blanket. The mice in the sham group underwent only an abdominal incision without cecum ligation or puncture. Each group consisted of 10 mice, following a specific intervention protocol. Five of these mice were observed for basic conditions and mortality for 7 days post-sepsis modelling, while the remaining 5 were used for sampling and subsequent experiments 24 hours after modelling. One hour and twelve hours post-modelling, the CLP_AuDAMP1, CLP_AuDAMP2, CLP_AuDAMP3, CLP_mlpn, and CLP_AuDAMP3_mlpn groups received intraperitoneal (IP) injections of the following drugs: AuDAMP at doses of 5 mg kg^{-1}, 10 mg kg^{-1}, and 20 mg kg^{-1}; meropenem at 20 mg kg^{-1}; and a combination of meropenem at 20 mg kg^{-1} and AuDAMP at 20 mg kg^{-1}. The sham and CLP groups received equal volumes of saline. Twenty-four hours after modelling, the mice were anesthetized, and samples were collected for analysis. Study 2: establishing and grouping the LPS-induced acute lung injury (ALI) model. The mice were divided into three groups: standard control (SC), acute lung ALI, and ALI_AuDAMP, with 5 mice per group. To establish the LPS-induced acute lung injury model, the following procedure was used: (1). The mice were anesthetized, and then the trachea was intubated. Successful intubation was confirmed when fluid dripping through the tracheal tube caused the mice to choke. (2). LPS (from *Escherichia coli* O55 : B5) was purchased from Sigma and was administered at a dose of 10 mg kg^{-1} through the tracheal tube to induce acute lung injury, whereas the SC group

received the same volume of saline. (3). One hour after the model was established, the ALI_AuDAMP group was treated with 5 mg kg^{-1} of AuDAMP. The SC and ALI groups received an equivalent volume of saline. (4). Twenty-four hours after modelling, the mice were anesthetized, and blood and lung tissues were collected for further analysis.

The modified murine sepsis score (MSS) was utilized to evaluate the severity of CLP-induced polymicrobial sepsis in mice.[28,29] The MSS assesses seven aspects: appearance, level of consciousness, activity, response to stimuli, eyes, respiratory rate, and quality of breath. Each aspect is rated on a scale ranging from 0 to 4, resulting in a total possible score of 28 for each mouse. Mice that succumb to the condition are assigned the maximum score. Each group was assessed and scored at intervals of 24, 48, 72, 96, 120, 144, and 168 hours after modeling. Twenty-four hours after modeling, the mice were anesthetized with tribromoethanol, and blood samples were collected. The blood was centrifuged at 3000 rpm for 10 minutes, and the supernatant was frozen for further analysis. The abdominal cavity was rinsed with 2 ml of sterile saline to obtain an abdominal rinse. The levels of LPS, IL-1β, IL-6, and TNF-α were measured *via* ELISA according to the instructions provided with kits from Andygene. These inflammatory markers were assessed in the serum and ascites of the CLP-induced sepsis model and in the serum and lung tissue of the ALI model. The levels of ALT and creatinine in the serum were measured with commercial kits from Jiancheng Bioengineering to assess hepatic and renal function in the mice. This analysis helped determine the extent of liver and kidney impairment in septic mice and evaluate whether high doses of AuDAMP are toxic to healthy mice.

Fifty microliters of the ascites were diluted 10^5 times and spread evenly on a 9 cm blood agar plate purchased from Huan Kai Biology, after which the plates were incubated in aerobic and anaerobic environments for 48 h, after which the number of colonies was counted. The total number of colonies (CFU mL^{-1}) = $N \times (1/0.05) \times 10^5$, where N is the number of colonies on the plate. Ascitic bacteria were also analyzed *via* 16S rRNA gene V3–V4 region sequencing, and the sequencing data were processed and analyzed with QIIME2 (V-2023.5.0, **https://www.qiime2.org/**) and R software (version 4.2.1, University of Auckland, New Zealand). In particular, unweighted UniFrac distances were utilized to evaluate differences in bacterial communities between groups.

Colon, liver, kidney, and lung tissues were washed with sterile saline and fixed in 4% paraformaldehyde for 24 hours. The tissues were then paraffin-embedded, sectioned at 3 μm, and analyzed under a microscope *via* hematoxylin–eosin (H&E) staining. Edema, necrosis, hemorrhage, and inflammatory cell infiltration were quantified in the colon, kidney, and liver tissues. These parameters were graded on a scale from 0 to 4, with 0 indicating "absent" and 4 indicating "severe".[30] The histological scores of the lung tissue were assessed on the basis of five pathological aspects: hemorrhage, the presence of neutrophils in the alveolar space, hyaline membrane formation, proteinaceous debris filling the airspaces, and septal thickening. Each aspect was evaluated to provide a comprehensive understanding of lung pathology.[31] The severity of lung tissue injury was graded on a scale from 0 to 4, with 0 indicating no injury, 1 indicating less than 25% injury, 2 indicating 25 to 50% injury, 3 indicating 50 to 75% injury, and 4 indicating more than 75% injury. The scores for the five pathological aspects were summed to provide an overall lung tissue injury score. To ensure accuracy in assessing lesions in the colon, liver, kidney, and lung, three pathologists, who were blinded to the experimental design, independently scored the tissues. The final score for each animal was calculated by averaging the scores given by the three pathologists.

After planning all the things, we employed the CLP-induced polymicrobial infection model in C57BL/6 male mice and divided them into groups treated with AuDAMP alone or in combination with meropenem. Meropenem is a carbapenem antibiotic that inhibits the synthesis of bacterial cell walls, thereby preventing bacterial growth and reproduction.[32] This approach aimed to investigate the antiseptic effects of our synthesized ultrasmall AuDAMP clusters and to determine whether they exhibit a synergistic antiseptic effect when combined with meropenem. The mice received intraperitoneal injections of the corresponding treatments at 1 hour and 12 hours post-modeling. Throughout the study, the mice were continuously monitored for characteristics related to the MSS, and their body weights were recorded. Additionally, mortality rates were tracked over a period of 7 days (Fig. 1A). Survival curves revealed that low-dose AuDAMP had minimal antiseptic effects, with all mice dying within two days post-modeling, showing survival outcomes almost indistinguishable from those in the CLP group. As the dose increased, the mice survived longer, and the group treated with AuDAMP combined with meropenem presented an antiseptic advantage, with mice surviving longer than those in the other groups; one mouse died on the second day (Fig. 1B). The modified MSS scores showed the same trend, with almost no therapeutic effect at 5 mg kg^{-1} and a gradual decrease as the dose of AuDAMP increased (Fig. 1C). There was a significant antiseptic advantage in the group treated with a high dose of AuDAMP combined with meropenem, showing the lowest MSS scores compared with the other treatment groups (Fig. 1C). The body weights of the mice in each group during the observation period almost continuously decreased for the first 72 hours after modeling and then slightly increased in the medium- and high-dose AuDAMP groups as well as the meropenem-treated groups (Fig. 1D). High-dose AuDAMP exhibited antiseptic effects, improved the MSS scores and body weights of CLP mice, and was more effective when combined with meropenem.

AuDAMP in combination with meropenem is more promising for restoring abdominal microorganisms in septic mice. AuDAMP exhibited antibacterial activity, as illustrated in Fig. 2A. Compared with the CLP group, the high dose of AuDAMP had significant antibacterial effects, resulting in a markedly lower number of bacterial colonies after 48 hours of incubation. When AuDAMP was combined with meropenem, significant antimicrobial synergism was observed, with nearly complete eradication of bacteria in the ascites. This antimicrobial effect was better than that in the groups treated with

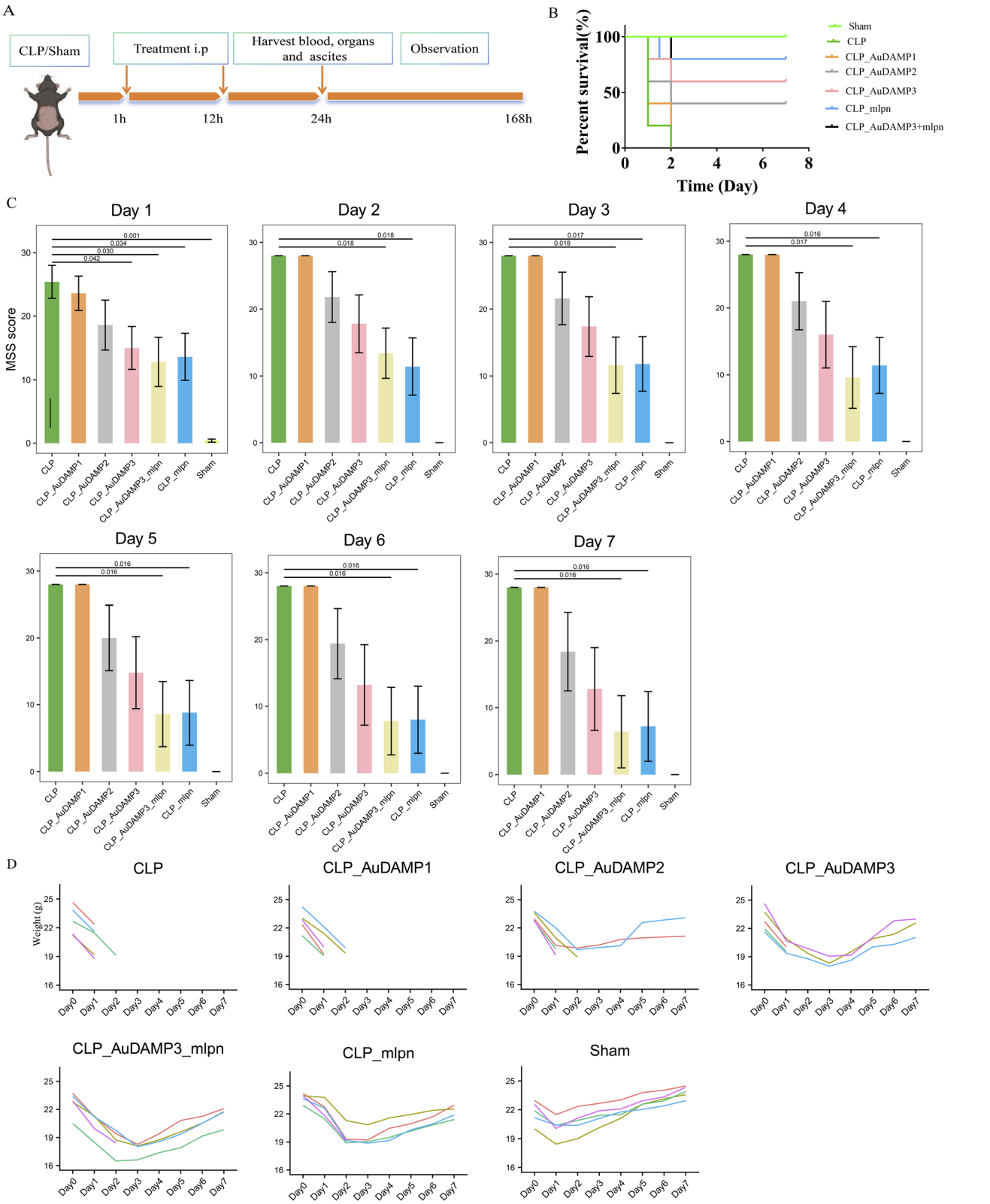

Fig. 1 Therapeutic efficacy of AuDAMP alone or in combination with meropenem in the CLP-induced sepsis model. (A) Experimental schedule for CLP-induced sepsis modeling of polymicrobial infections. (B) Survival curves of the mice during observation. (C) MSS scores from days 1 to 7 in each group. (D) Body weights of the mice in each group during the observation period. Each group included 5 samples, and the abbreviation "mlpn" in the figure represents "meropenem".

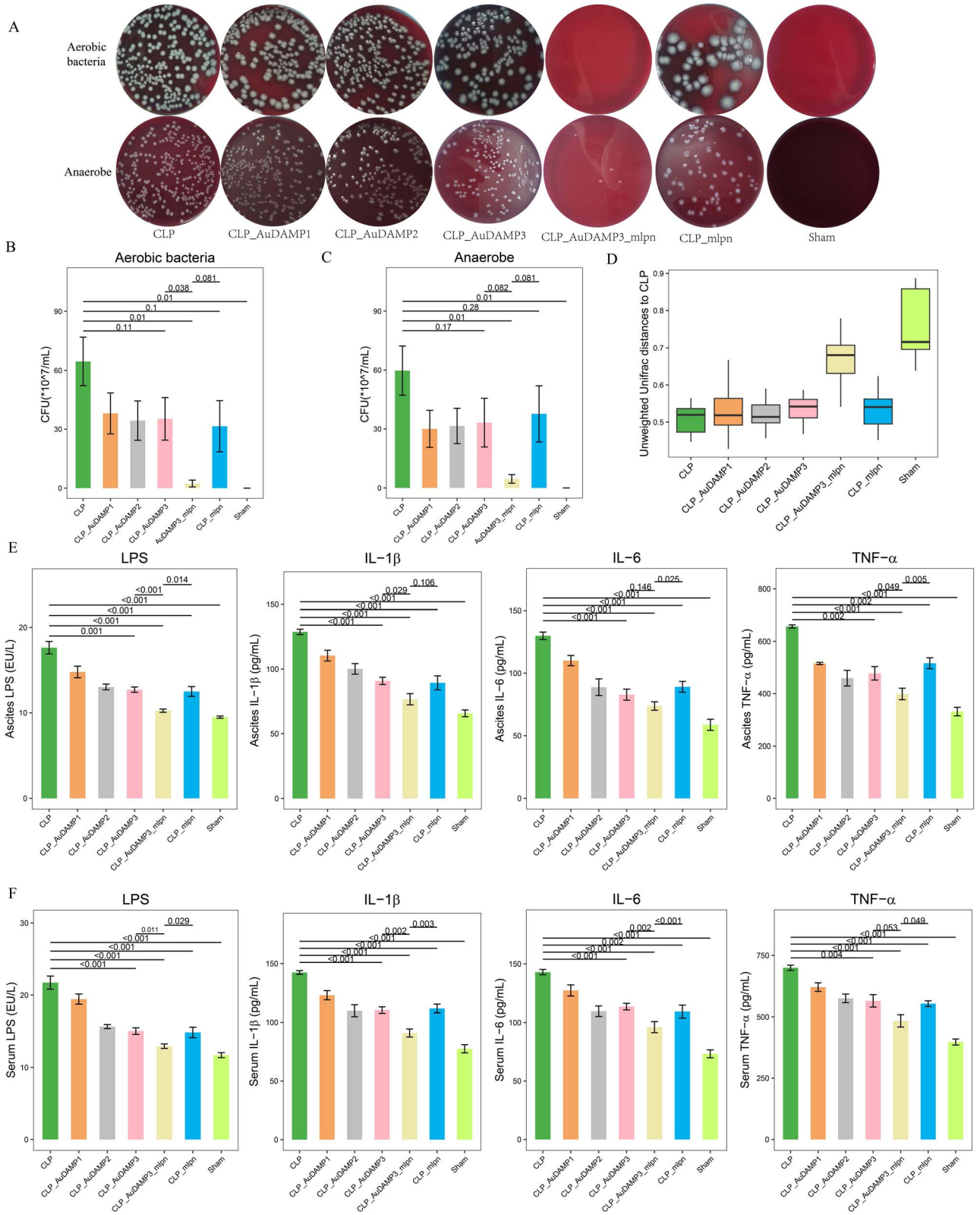

Fig. 2 Antimicrobial and cytokine-scavenging efficacy of AuDAMP alone or in combination with meropenem in a CLP-induced sepsis model. (A) Colony formation of ascitic bacteria cultured in anaerobic and aerobic environments for 48 hours. (B) Histogram of the quantitative statistics of the number of colonies formed by aerobic bacteria in (A). (C) Histogram of the quantitative statistics of the number of colonies formed by anaerobes in (A). (D) Boxplot of unweighted UniFrac distance statistics for each group based on 16S rRNA sequencing data analysis. (E) Levels of LPS, IL-1β, IL-6, and TNF-α in the ascites of the mice. (F) Serum levels of LPS, IL-1β, IL-6, and TNF-α in the mice. Each group consisted of 5 samples.

AuDAMP alone or meropenem alone (Fig. 2A). The results for anaerobic bacteria were consistent with those for aerobic bacteria (Fig. 2B and C). Our previous study showed that the combination of AuDAMP with daptomycin also exhibited a synergistic antibacterial effect.[33] AuDAMP kills bacteria through several mechanisms, including disrupting bacterial cell membranes, damaging bacterial DNA, promoting the generation of reactive oxygen species (ROS), and impairing bacterial growth and reproduction.[13] It could kill not only extracellular bacteria but also intracellular bacteria. Our preliminary research demonstrated its effectiveness in eliminating methicillin-resistant *Staphylococcus aureus* (MRSA) from macrophages.[21] Additionally, the results of 16S rRNA sequencing analysis, using unweighted UniFrac distance, indicated that the bacterial communities in the ascites from the AuDAMP combined with meropenem treatment group were far from those of the CLP group but closely resembled those of the sham group (Fig. 2D). Our results demonstrated that the combination of AuDAMP and meropenem exhibits antimicrobial synergy. With the widespread use of antibiotics, the prevalence of resistant bacteria is increasing, making effective control of such bacterial infections a significant challenge for clinicians.[34] Engineered nanostructures with high specific surface areas and exceptional antimicrobial performance represent one of the most promising classes of antimicrobial agents, as microorganisms may have difficulty developing resistance to them.[35] It has been reported that nanomaterials can be combined with manganese and antibiotics to create new nanoantibiotics, which have significant therapeutic effects in the treatment of sepsis.[14] If new nanoantibiotics are developed by combining AuDAMP with antibiotics or other antimicrobial agents while retaining the beneficial properties of the nanoparticles, they may effectively penetrate cells without being recognized and expelled by resistant bacteria.[33] This approach could lead to the development of innovative nanoantibiotics, offering new hope in the fight against super-resistant bacteria. This is the direction we aim to pursue in our future research.

LPS, a major inflammatory mediator and a key component of the cell wall of Gram-negative bacteria, plays a significant role in this process. It activates the immune system, leading to hyperinflammation, cytokine storms, microcirculatory disturbances, and ultimately death.[36] Reducing LPS levels effectively controls cytokine storms and mitigates inflammatory damage in sepsis. The combination of AuDAMP and meropenem effectively eliminates bacteria, inhibits bacterial growth and reproduction, and blocks the cascade release of LPS. AuDAMP also effectively scavenges LPS and cytokines (IL-1β, IL-6, and TNF-α) in both ascites and serum (Fig. 2E and F). Compared with the CLP group, the levels of LPS and cytokines in the ascites and serum of the high-dose AuDAMP combined with meropenem group were significantly lower. Furthermore, the combination of AuDAMP and meropenem was more effective at scavenging inflammatory mediators and cytokines than either AuDAMP or meropenem alone. Thus, AuDAMP can effectively reduce the level of free LPS both by blocking the source of LPS through its bactericidal action and by binding to negatively charged free LPS, thereby attenuating cytokine storms and reducing inflammatory damage. Li, Z., Feng, *et al.* also reported that nanoparticles can remove inflammatory mediators.[14]

The pathology of acute inflammatory damage to organs is characterized by five aspects, as previously mentioned. Compared with CLP, 20 mg kg^{-1} AuDAMP significantly reduced organ damage. Histological analysis *via* H&E staining revealed preservation of the normal tissue structure, with no infiltration of neutrophils and only slight edema observed (Fig. 3A). Furthermore, the combination of AuDAMP and meropenem resulted in less organ damage than other treatments. The histogram of organ pathology scores indicated that AuDAMP effectively attenuated the organ damage associated with sepsis, indicating an increasing trend toward protection with increasing doses of AuDAMP (Fig. 3B). The combination of AuDAMP and meropenem provided the most substantial protection against organ damage induced by sepsis. Biochemical indicators of liver and kidney function, specifically ALT and creatinine levels, also demonstrated a dose-dependent protective effect of AuDAMP. The highest dose of AuDAMP, particularly in combination with meropenem, had the strongest protective effect, as illustrated in Fig. 3C and D, which aligns with the histopathology scores.

To assess the potential toxicity of high doses of AuDAMP in normal mice, 20 mg kg^{-1} of AuDAMP was administered *via* intraperitoneal injection for 7 days, and ALT and creatinine levels were evaluated. Fig. S2A and B† show the levels of ALT and creatinine in the serum, respectively, indicating that a high dose of AuDAMP does not impair organ function.

Dripping LPS *via* intratracheal administration is a classical model for studying LPS-induced acute lung injury and was used to validate the ability of AuDAMP to scavenge LPS and cytokines. Fig. 4A illustrates the schedule for LPS-induced acute lung injury. AuDAMP was administered 1 hour after LPS instillation. H&E staining of lung tissue from the LPS-induced acute lung injury model revealed alveolar hemorrhage, inflammatory cell infiltration, and proteinaceous debris filling the airspaces. Notably, AuDAMP significantly attenuated inflammatory injury in the lung tissue (Fig. 4B). Analysis of lung histopathology scores confirmed that AuDAMP protected against LPS-induced lung injury (Fig. 4B). Furthermore, as shown in Fig. 4C and D, AuDAMP significantly reduced the levels of LPS and cytokines such as IL-1β, IL-6, and TNF-α in both lung tissue and serum. These findings indicate that AuDAMP mitigates the cytokine storm by decreasing free LPS levels, thereby exerting anti-inflammatory and organ-protective effects.

Our results demonstrated that AuDAMP decreased the levels of LPS and cytokines in both the serum and ascites in the CLP-induced sepsis model, as well as in the serum and lung tissue in the LPS-induced lung injury model. Furthermore, we observed that the combination of AuDAMP with meropenem resulted in a more significant reduction in free LPS in the sepsis model, likely due to the enhanced bactericidal effect of the combination.

In summary, the synthesized Au NCs (AuDAMP) can effectively scavenge LPS and attenuate cytokine storms, thereby exerting antiseptic effects. In addition to its antimicrobial

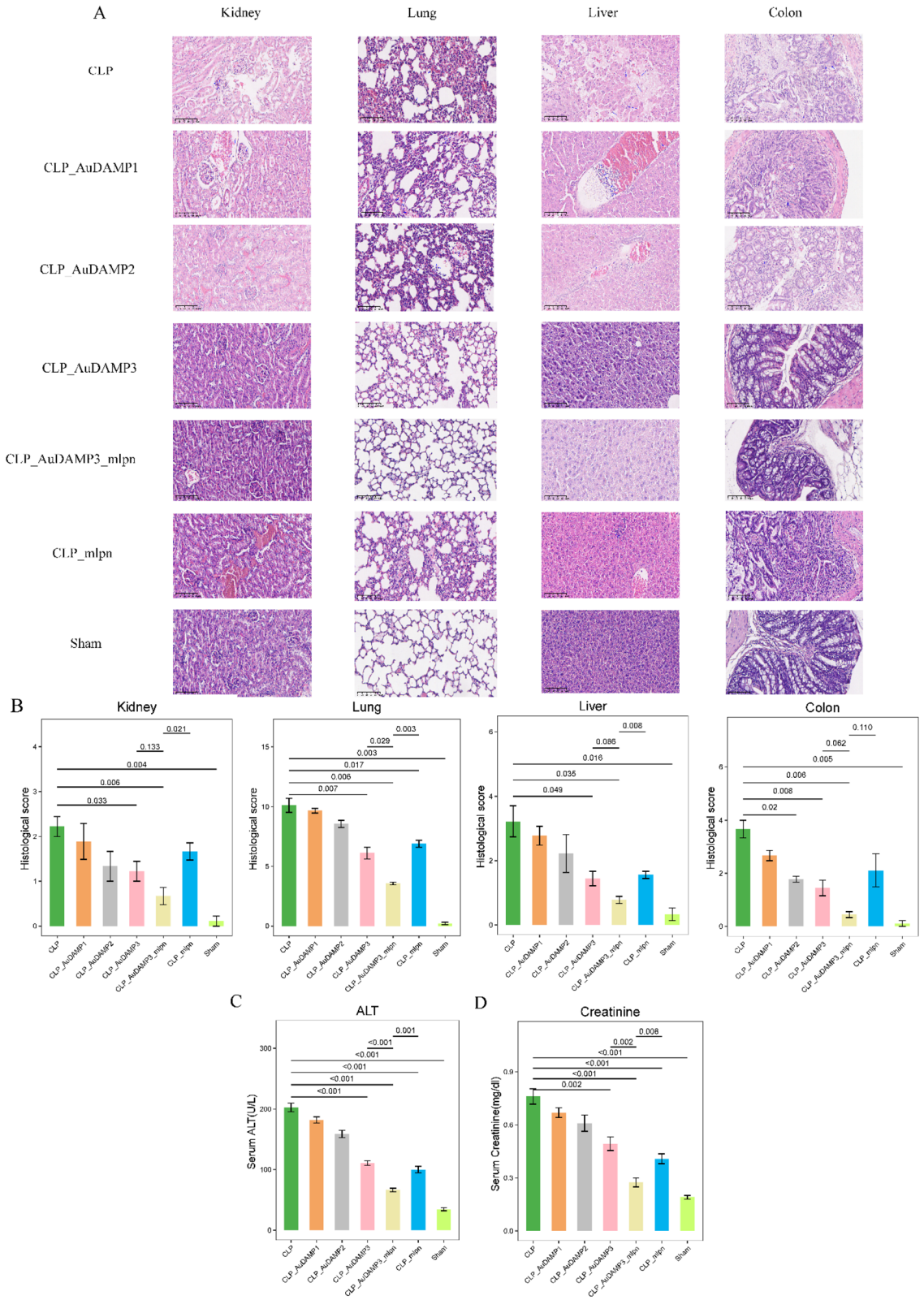

Fig. 3 Pathologic damage to organs in each group. (A) H&E staining of colon, liver, lung, and kidney tissues from each group (200×). Scale bar = 100 μm. The blue arrows in the figure indicate neutrophils ($n = 3$). (B) Histograms of H&E-stained pathological scores of the colons, liver, lungs, and kidneys in each group. (C) Histograms of the levels of ALT in each group. (D) Histograms of the levels of creatinine in each group; 3 samples per group were used for pathological tests, and 5 samples were used for other tests.

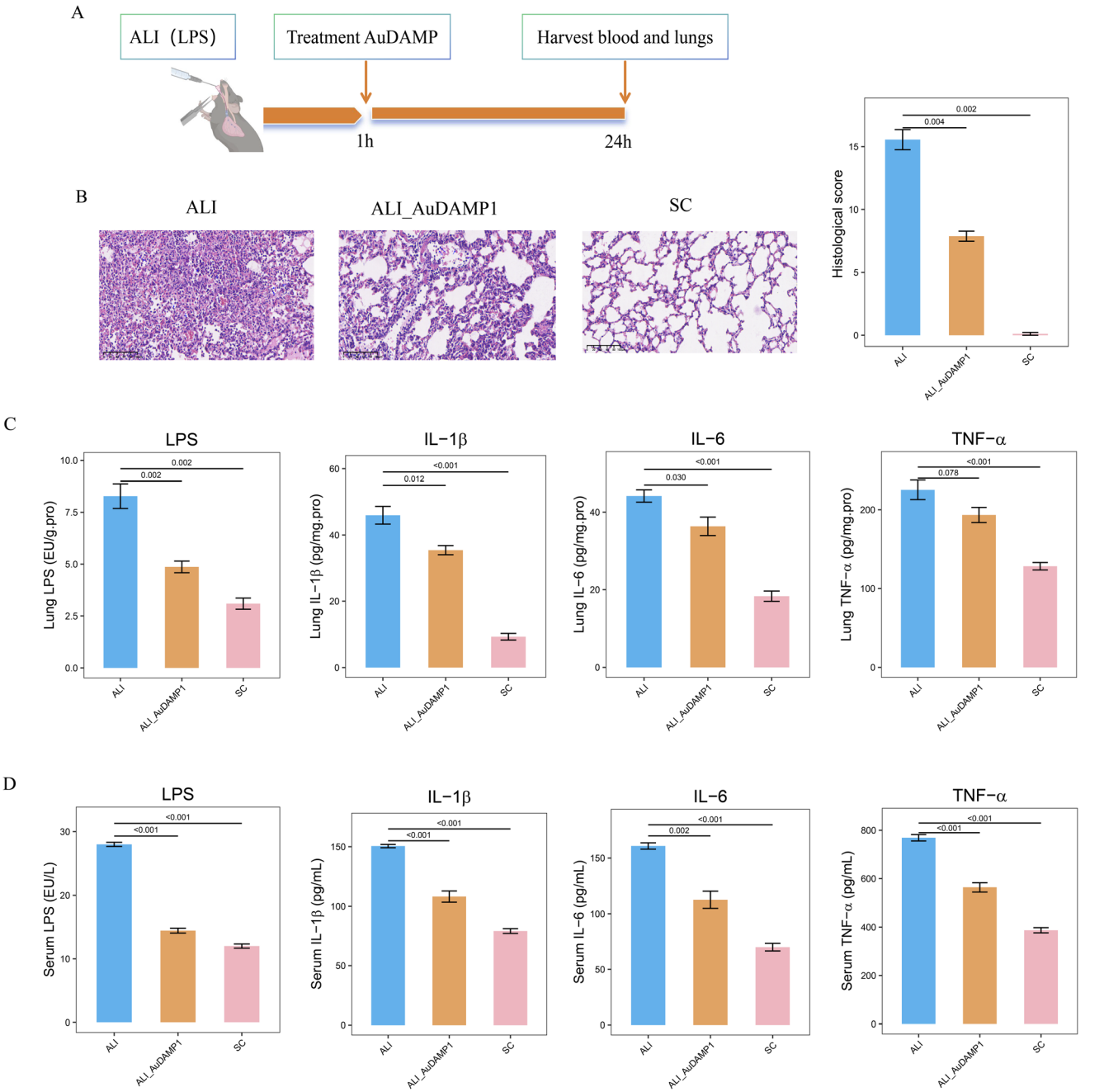

Fig. 4 Therapeutic effects of AuDAMP in an LPS-induced lung injury model. (A) Experimental schedule for LPS-induced acute lung injury. (B) H&E staining of lung tissues from each group; blue arrows indicate neutrophils (200×, scale bar = 100 μm), and a histogram of the results of the quantitative analysis of their pathology scores is shown. (C) The levels of LPS, IL-1β, IL-6, and TNF-α in the lung tissue of each group. (D) Serum levels of LPS, IL-1β, IL-6, and TNF-α.

properties, AuDAMP removes major inflammatory mediators and demonstrates synergistic antimicrobial activity when combined with meropenem. These attributes provide promising potential for the treatment of severe sepsis and infections caused by drug-resistant bacteria.

Ethical approval

Ethical approval was given by the Animal Ethics Committee of Southwest Medical University (SWMU.20240040).

Data availability

The data supporting this article have been included as part of the ESI.†

Author contributions

Chengli Wen: writing-review and editing, writing-original draft, visualization, methodology, formal analysis, data curation, conceptualization, and funding acquisition. Youkun Zheng:

methodology, data curation, writing-original draft, and funding acquisition. Yong Li: methodology, data curation. Liping Yuan: methodology. Sicheng Liang: investigation, conceptualization; Xianying Lei: methodology, formal analysis. Tao Xu: conceptualization. Muhan Lü: conceptualization, project administration, supervision, writing-review and editing, and funding acquisition. Wanmeng Xiao: conceptualization, project administration, supervision, writing-review and editing, and funding acquisition. Zehui Yu: conceptualization, project administration, supervision, writing-review and editing.

Conflicts of interest

No potential conflicts of interest were disclosed.

Acknowledgements

The study was funded by the Sichuan Science and Technology Program (grant number: 2022YFS0626), the Natural Science Foundation of Sichuan Province (grant number: 2024NSFSC2104), Southwest Medical University and Xuyong County People's Hospital (grant number: 2023XYXNYD16), Luzhou Municipal People's Government and Southwest Medical University (grant number: 2023LZXNYDJ001), and the Doctoral Research Initiation Fund of the Affiliated Hospital of Southwest Medical University. I would like to thank the undergraduate students of Southwest Medical University, Ye-wei Su, Cheng-Xiang Lin, and Jing-fan Zheng for their help during my experiment.

References

1 M. Singer, C. S. Deutschman, C. W. Seymour, M. Shankar-Hari, D. Annane, M. Bauer, R. Bellomo, G. R. Bernard, J. D. Chiche, C. M. Coopersmith, R. S. Hotchkiss, M. M. Levy, J. C. Marshall, G. S. Martin, S. M. Opal, G. D. Rubenfeld, T. van der Poll, J. L. Vincent and D. C. Angus, *JAMA*, 2016, **315**, 801–810.

2 L. Evans, A. Rhodes, W. Alhazzani, M. Antonelli, C. M. Coopersmith, C. French, F. R. Machado, L. McIntyre, M. Ostermann, H. C. Prescott, C. Schorr, S. Simpson, W. J. Wiersinga, F. Alshamsi, D. C. Angus, Y. Arabi, L. Azevedo, R. Beale, G. Beilman, E. Belley-Cote, L. Burry, M. Cecconi, J. Centofanti, A. Coz Yataco, J. De Waele, R. P. Dellinger, K. Doi, B. Du, E. Estenssoro, R. Ferrer, C. Gomersall, C. Hodgson, M. H. Møller, T. Iwashyna, S. Jacob, R. Kleinpell, M. Klompas, Y. Koh, A. Kumar, A. Kwizera, S. Lobo, H. Masur, S. McGloughlin, S. Mehta, Y. Mehta, M. Mer, M. Nunnally, S. Oczkowski, T. Osborn, E. Papathanassoglou, A. Perner, M. Puskarich, J. Roberts, W. Schweickert, M. Seckel, J. Sevransky, C. L. Sprung, T. Welte, J. Zimmerman and M. Levy, *Intensive Care Med.*, 2021, **47**, 1181–1247.

3 Y. Li, H. Zhang, C. Chen, K. Qiao, Z. Li, J. Han, X. Han, K. Li, K. Lai, N. Liu, A. Li, N. Xiao, Y. Zhang, X. Zhao, W. Gao, Y. Zhang, H. Liu and T. Sun, *Adv. Mater.*, 2022, **34**, e2108476.

4 C. R. Donnelly, O. Chen and R. R. Ji, *Trends Neurosci.*, 2020, **43**, 822–838.

5 E. J. Giamarellos-Bourboulis, A. C. Aschenbrenner, M. Bauer, C. Bock, T. Calandra, I. Gat-Viks, E. Kyriazopoulou, M. Lupse, G. Monneret, P. Pickkers, J. L. Schultze, T. van der Poll, F. L. van de Veerdonk, A. P. J. Vlaar, S. Weis, W. J. Wiersinga and M. G. Netea, *Nat. Immunol.*, 2024, **25**, 19–28.

6 X. Mu and S. Hur, *Acc. Chem. Res.*, 2021, **54**, 4012–4023.

7 A. T. Ngo, A. Skidmore, J. Oberg, I. Yarovoi, A. Sarkar, N. Levine, V. Bochenek, G. Zhao, L. Rauova, M. A. Kowalska, K. Eckart, N. S. Mangalmurti, A. Rux, D. B. Cines, M. Poncz and K. Gollomp, *JCI Insight*, 2023, **8**, e171054.

8 C. Kim, H. Sim and J. S. Bae, *Int. J. Mol. Sci.*, 2022, **23**, 13130.

9 M. Huemer, S. Mairpady Shambat, S. D. Brugger and A. S. Zinkernagel, *EMBO Rep.*, 2020, **21**, e51034.

10 M. Ye, Y. Zhao, Y. Wang, R. Xie, Y. Tong, J. D. Sauer and S. Gong, *Nat. Nanotechnol.*, 2022, **17**, 880–890.

11 D. P. Schrijver, R. J. Röring, J. Deckers, A. de Dreu, Y. C. Toner, G. Prevot, B. Priem, J. Munitz, E. G. Nugraha, Y. van Elsas, A. Azzun, T. Anbergen, L. A. Groh, A. M. D. Becker, C. Pérez-Medina, R. S. Oosterwijk, B. Novakovic, S. Moorlag, A. Jansen, P. Pickkers, M. Kox, T. J. Beldman, E. Kluza, M. M. T. van Leent, A. J. P. Teunissen, R. van der Meel, Z. A. Fayad, L. A. B. Joosten, E. A. Fisher, M. Merkx, M. G. Netea and W. J. M. Mulder, *Nat. Biomed. Eng.*, 2023, **7**, 1097–1112.

12 C. Tang, W. Jing, K. Han, Z. Yang, S. Zhang, M. Liu, J. Zhang, X. Zhao, Y. Liu, C. Shi, Q. Chai, Z. Li, M. Han, Y. Wang, Z. Fu, Z. Zheng, K. Zhao, P. Sun, D. Zhu, C. Chen, D. Zhang, D. Li, S. Ni, T. Li, J. Cui and X. Jiang, *ACS Nano*, 2024, **18**, 2261–2278.

13 Y. Zheng, W. Liu, Z. Qin, Y. Chen, H. Jiang and X. Wang, *Bioconjugate Chem.*, 2018, **29**, 3094–3103.

14 Z. Li, Y. Feng, S. Zhang, T. Li, H. Li, D. Wang, K. Hao, C. He, H. Tian and X. Chen, *ACS Nano*, 2023, **17**, 8551–8563.

15 L. Papafilippou, A. Claxton, P. Dark, K. Kostarelos and M. Hadjidemetriou, *Adv. Healthcare Mater.*, 2021, **10**, e2001378.

16 C. Lu, L. Xue, K. Luo, Y. Liu, J. Lai, X. Yao, Y. Xue, W. Huo, C. Meng, D. Xia, X. Gao, Q. Yuan and K. Cao, *ACS Nano*, 2023, **17**, 18421–18432.

17 Y. Gong, X. Zhao, X. Yan, W. Zheng, H. Chen and L. Wang, *J. Colloid Interface Sci.*, 2024, **674**, 490–499.

18 B. Casteleiro, J. M. G. Martinho and J. P. S. Farinha, *Nanoscale*, 2021, **13**, 17199–17217.

19 K. Zheng, M. I. Setyawati, D. T. Leong and J. Xie, *ACS Nano*, 2017, **11**, 6904–6910.

20 K. Zheng, M. I. Setyawati, D. T. Leong and J. Xie, *Bioact. Mater.*, 2021, **6**, 941–950.

21 Z. Tang, S. Liu, N. Chen, M. Luo, J. Wu and Y. Zheng, *Colloids Surf., B*, 2021, **205**, 111899.

22 F. H. Liao, T. H. Wu, Y. T. Huang, W. J. Lin, C. J. Su, U. S. Jeng, S. C. Kuo and S. Y. Lin, *Nano Lett.*, 2018, **18**, 2864–2869.

23 Y. Zhao, Y. Tian, Y. Cui, W. Liu, W. Ma and X. Jiang, *J. Am. Chem. Soc.*, 2010, **132**, 12349–12356.
24 Y. Zheng, W. Liu, Y. Chen, H. Jiang and X. Wang, *J. Mater. Chem. B*, 2018, **6**, 3650–3654.
25 Y. Xie, Y. Liu, J. Yang, Y. Liu, F. Hu, K. Zhu and X. Jiang, *Angew Chem. Int. Ed. Engl.*, 2018, **57**, 3958–3962.
26 C. N. Loynachan, A. P. Soleimany, J. S. Dudani, Y. Lin, A. Najer, A. Bekdemir, Q. Chen, S. N. Bhatia and M. M. Stevens, *Nat. Nanotechnol.*, 2019, **14**, 883–890.
27 A. O. Frimpong, X. Xu, X. Jia and Y. Zhang, *J. Chem. Phys.*, 2022, **157**, 154902.
28 S. H. Kathem, Y. S. Nasrawi, S. H. Mutlag and S. M. Nauli, *Biomolecules*, 2024, **14**, 334.
29 B. Shrum, R. V. Anantha, S. X. Xu, M. Donnelly, S. M. Haeryfar, J. K. McCormick and T. Mele, *BMC Res. Notes*, 2014, **7**, 233.
30 H. Liang, H. Song, X. Zhang, G. Song, Y. Wang, X. Ding, X. Duan, L. Li, T. Sun and Q. Kan, *Emerging Microbes Infect.*, 2022, **11**, 815–828.
31 H. H. Yang, J. X. Duan, S. K. Liu, J. B. Xiong, X. X. Guan, W. J. Zhong, C. C. Sun, C. Y. Zhang, X. Q. Luo, Y. F. Zhang, P. Chen, B. D. Hammock, S. H. Hwang, J. X. Jiang, Y. Zhou and C. X. Guan, *Theranostics*, 2020, **10**, 4749–4761.
32 D. Shah and M. Narang, *Indian Pediatr.*, 2005, **42**, 443–450.
33 Y. Zheng, W. Liu, Y. Chen, C. Li, H. Jiang and X. Wang, *J. Colloid Interface Sci.*, 2019, **546**, 1–10.
34 J. Ma, X. Song, M. Li, Z. Yu, W. Cheng, Z. Yu, W. Zhang, Y. Zhang, A. Shen, H. Sun and L. Li, *Microbiol. Res.*, 2023, **266**, 127249.
35 M. S. Ahmed, T. Annamalai, X. Li, A. Seddek, P. Teng, Y. C. Tse-Dinh and J. H. Moon, *Bioconjugate Chem.*, 2018, **29**, 1006–1009.
36 K. Dickson and C. Lehmann, *Int. J. Mol. Sci.*, 2019, **20**, 4341.